Proceedings of ASME Turbo Expo 2011
GT2011
June 6-10, 2011, Vancouver, British Columbia, Canada

GT2011-45874

EXPERIMENTAL INVESTIGATION OF TURBINE STATOR WELL RIM SEAL, RE-INGESTION AND INTERSTAGE SEAL FLOWS USING GAS CONCENTRATION TECHNIQUES AND DISPLACEMENT MEASUREMENTS

D. Eastwood[1], D. D. Coren, C. A. Long, N. R. Atkins[2]
Thermo-Fluid Mechanics Research Centre, University of Sussex, Brighton, BN1 9QT, UK

P. R. N. Childs
Dept. of Mech. Engineering
Imperial College London
South Kensington
London, SW7 2AZ, UK

T. J. Scanlon, A. Guijarro-Valencia
Thermal Systems
Rolls-Royce plc
Derby, UK

ABSTRACT

Gas turbine engine performance requires effective and reliable internal cooling over the duty cycle of the engine. Life predictions for rotating components subject to the main gas path temperatures are vital. This demands increased precision in the specification of the internal air system flows which provide turbine stator well cooling and sealing. This in turn requires detailed knowledge of the flow rates through rim seals and interstage labyrinth seals. Knowledge of seal movement and clearances at operating temperatures is of great importance when prescribing these flows. A test facility has been developed at the University of Sussex, incorporating a two stage turbine rated at 400 kW with an individual stage pressure ratio of 1.7:1. The mechanical design of the test facility allows internal cooling geometry to be rapidly re-configured, while cooling flow rates of between 0.71 $C_{W,\ ENT}$ and 1.46 $C_{W,\ ENT}$, may be set to allow ingress or egress dominated cavity flows. The main annulus and cavity conditions correspond to in cavity rotational Reynolds numbers of $1.71\text{x}10^6 < Re_\varphi < 1.93\text{x}10^6$. Displacement sensors have been used to establish hot running seal clearances over a range of stator well flow conditions, allowing realistic flow rates to be calculated. Additionally, gas seeding techniques have been developed, where stator well and main annulus flow interactions are evaluated by measuring changes in gas concentration. Experiments have been performed which allow rim seal and re-ingestion flows to be quantified. It will be shown that this work develops the measurement of stator well cooling flows and provides data suitable for the validation of improved thermo-mechanical and CFD codes, beneficial to the engine design process.

NOMENCLATURE

a	disc inner radius [m]
A_{SEAL}	circumferential seal area [m^3]
b	disc outer radius [m]
C_D	seal discharge coefficient
$\dot{m}$	mass flow rate [kg s^{-1}]
P	static pressure [Pa]
P_0	total pressure [Pa]
r	local radius [m]
R	gas constant for air [J kg^{-1} K^{-1}]
s	axial rotor-stator spacing [m]
T	static temperature [K]
T_o	total temperature [K]
μ	dynamic viscosity [kg m^{-1} s^{-1}]
v_φ	tangential velocity component [ms^{-1}]
ρ	density [kg m^{-3}]
γ	ratio of specific heats
ω	rotational speed [rad s^{-1}]

Dimensionless

$C_{W,}$	non-dimensional throughflow, $m\ b^{-1}\mu^{-1}$
Re_φ	rotational Reynolds number, $\rho\omega r^2\mu^{-1}$
β	swirl ratio, $v_\varphi\ r\omega^{-1}$

Subscripts

0	free disc flow value
1	upstream of interstage seal
2	downstream of interstage seal
C	cooling air
EGR	rim seal egress
ENT	disk with inner hub flow value
ING	rim seal ingress
IS	interstage seal flow
RE	re-ingested flow
SC	seeded cooling air
SG	seeding gas
SW	stator well (either up or downstream)
USW	upstream stator well
WS	wheel space

Abbreviations

CFD	computational fluid dynamics
DR	dilution ration
GC	gas concentration
NDIR	non-dispersive infrared sensor

[1]Correspondence to de23@sussex.ac.uk
[2]Now at the Whittle Laboratory. University of Cambridge

INTRODUCTION

The prevention of hot main stream gas ingress through turbine rim seals is of great interest to gas turbine manufacturers. Hot gas ingestion through rim seals into disc cavities can lead to the overheating of discs, reducing component life. It is commonly necessary to provide cool sealing air to the disc cavities to prevent or limit this ingestion of hot main annulus gas. The necessary coolant flow rate is governed by flows prevalent to stator wells and the exchange of the stator well flows with the main annulus flows at the rim seal. The cooling air is supplied from various compressor bleed locations. Since this directly affects the cycle performance it is important that the sealing air required to prevent ingestion is minimised.

This paper discusses the use of gas concentration (GC) measurement techniques together with direct seal clearance measurements. The work is part of continuing investigations using the multi-configuration Turbine Stator Well (TSW) test facility at the Thermo-Fluid Mechanics Research Centre (TFMRC) at the University of Sussex. It is part of the EU FP6 MAGPI (Main Annulus Gas Path Interactions) programme, which has the purpose of improving the understanding of interactions between cooling and main stream flows.

The TSW facility at the University of Sussex was developed to study the interaction of stator well cooling and main annulus air. A detailed overview of the test facility is described by Coren *et al.* [1]. The rig can be run at engine representative conditions with a number of stator well geometries, allowing coolant delivery path and flow rate to be investigated. In addition to the gas concentration instrumentation discussed within this paper, the rig includes a high density of temperature and pressure instrumentation.

The results from two distinct GC experiments are discussed. The first set of experiments looks at gas path interaction in the vicinity of the rim-seals by quantifying the net ingestion of main annulus flow into the upstream stator well cavity. This was carried out across a range of cooling flows and delivery geometry. The second was conducted to obtain measurements to confirm the presence of cool upstream wheelspace flows being re-ingested into stator well cavities downstream. In support of these tests two displacement sensors have been installed which allows a FEA model to be validated, which enables the calculation of hot geometry.

These measurements enhance the understanding of the complex flows within the stator well and the exchange between the cooling air and main annulus air. This supports validation of the next generation of conjugate coupled models to be used for the optimisation of internal cooling systems.

REVIEW OF FLOWS

The stator well flow field comprises disc entrainment, rotor stator core flow, coolant, rim seal exchange and interstage seal flow. A schematic of these flows is shown in Figure 1. In a rotor stator configuration where $s/b > 0.1$ the rotor and stator can be assumed to have separate boundary layers with a 2D core which rotates. Daily and Nece [2] showed that the swirl ratio, β, is in the region of 0.4 relative to the rotor. Chew [3] provides a relationship (equation 3) which allows the flow entrained by a partial disc $C_{W,\,ENT}$ to be related to the free disc entrainment $C_{W,0}$ (equation 2) as demonstrated by Dorfman [4]. This is useful for the TWS rig arrangement where the drive arm can be considered a disc hub.

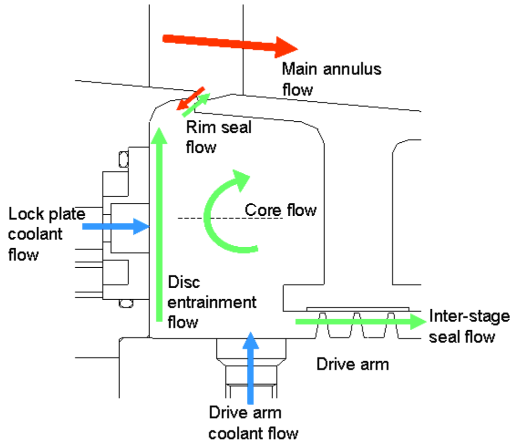

Figure 1: Stator well flow structure

The introduction of coolant into a stator well has a significant influence on the flow structure. In the Sussex TSW rig coolant may be introduced through either drive arm holes or bled through simulated lock plate slots. For the purpose of this paper cooling flows are given as a fraction of the disc entrainment $C_{W,\,ENT}$. Rotational Reynolds number is defined in equation 1. The density is calculated from the temperature and static pressure taken at a radius r = 0.905b, corresponding to the mid height of the upstream rotor stator cavity.

$$Re_{\varphi} = \frac{\rho\omega b^2}{\mu} \quad \textbf{Equation 1}$$

$$C_{W,O} = 0.219\ Re_{\varphi}^{0.8} \quad \textbf{Equation 2}$$

$$C_{W,ENT} = C_{W,O}\left[1-\left[\frac{a}{b}\right]^5\right] \quad \textbf{Equation 3}$$

Where:

$C_{W,ENT}$ = *Flow entrained by a disc with inner hub*

$C_{W,o}$ = *Flow entrained by a free disc*

a and b are the inner and outer disc radii

The flow of coolant, in particular the drive arm holes, due to their low radius entry into the stator, can affect the interstage seal inlet pressure and velocity. For cases where the supplied cooling flow is less than the disc entrainment value, the stator flows are in general dominated by entrainment flows and the interstage seal flow. As the coolant flow rate increases and becomes greater than the entrainment rate the stator flows become increasingly dominated by the resulting changes in core flow. Owen and Phadke [5] developed a correlation relating sealing coolant supply rates to main annulus conditions for a variety of rim seal geometries.

Interstage seals are used to reduce the flow of air from upstream to downstream stator wells. The seal flow is largely influenced by clearance value and the pressure drop across the seal which is a function of the upstream and downstream conditions including the pressure drop over the stage in the main annulus. The seal flow is calculated using the St. Venant-Wantzell equation for the ideal flow together with a single discharge coefficient, C_D, which accounts for all of the dependent parameters.

$$\dot{m} = C_D \frac{P_1 A}{\sqrt{T_0}} \left(\frac{P_2}{P_1}\right)^{\frac{1}{\gamma}} \sqrt{\frac{2\gamma}{R(\gamma-1)}\left[1-\left(\frac{P_2}{P_1}\right)^{\frac{\gamma-1}{\gamma}}\right]}$$

Equation 4

Zimmerman and Wolff [6], Gamal and Vance [7] and Wittig *et al* [8] provided seal discharge coefficients for a number of seal clearances, geometries and pressure ratios.

Rim seal flows are influenced by both the pressure drop across a stage as well as the seal geometry and pressure drop across the interstage seal. Circumferential pressure asymmetries in the main annulus which result from the flows associated with the blade rows can also have a large influence on rim seal flows. This effect was shown by Gentilhomme *et al.* [9]. The effect of the re-ingestion of cooling air from upstream cavities was investigated by Georgakis *et al*. [10]. It was shown that re-ingestion of upstream egress provided significant contribution to stator well cooling, which was quantified as improving thermal effectiveness on the downstream cavity walls.

PREVIOUS GAS CONCENTRATION STUDIES

Phadke and Owen [11] conducted studies of a rotor-stator system with seven distinct rim seal geometries, including axial, radial and mitred seals. The seals were tested over a range of clearance ratios and rotational Reynolds numbers. Tracer gas, nitrous oxide, could be supplied to the rig through either the cooling flow, or to the external air outside the rim seal. In order to measure the minimum amount of cooling air required to seal the rotor-stator wheelspace, the cooling air was supplied with a known concentration of nitrous oxide. The rotational speed of the rig was then increased while keeping the coolant flow constant, until the concentration was seen to drop. This was considered to be due to the ingress of air into the wheelspace, and indicated the point at which the supplied cooling air was insufficient to seal the wheelspace.

Dadkhah *et al* [12] conducted gas concentration experiments on two engine representative seals, one where the wheelspace is upstream of a rotor and a second where the wheelspace is downstream of a rotor. Gas concentration measurements where made via a traverse within the wheelspace at four radial locations, r = 0.163b, 0.411b, 0.658b, 0.905b, using nitrous oxide as a tracer gas seeded into the cooling air. The concentration measurements were used to determine the amount of main annulus gas ingested as well as the distribution of the ingested gas in the wheelspace. The study showed that where ingestion was present, the ingested gas entering the wheelspace was entrained onto the stator, where it then proceeded downwards. The ingested gas then moved across the core of the wheelspace into the rotor boundary layer. The study also showed that the highest dilution levels occurred at the higher radius of the wheelspace. Ingress mass flows were estimated by integration of the mean gas concentration levels.

As part of an investigation into ingestion through rim seals, Gentilhomme *et al*. [9] seeded cooling air with nitrous oxide and carbon dioxide and then made concentration measurements within the stator well. The results were compared to unsteady CFD solutions and a basic ingestion model. It was also shown through gas concentration results that the ratio of seal to annulus flow velocity was useful when correlating ingestion rates.

Green and Turner [13] used gas concentration techniques to investigate ingestion into the upstream wheelspace of an axial turbine. Using nitrous oxide as a tracer, gas concentration measurements were used together with pressure measurements to determine the level and distribution of ingestion. It was found that ingestion was present, even at sealing flow rates where the supplied sealing flow was greater than the disc entrainment.

Dunn *et al* [14] used measurements of concentration, static pressure and velocity together with numerical simulation to investigate the flow fields in a single-stage model air turbine rotor-stator cavity. Results showed circumferential static pressure variation in the main annulus caused by large scale flow structures directly affected the rim seal flow structure.

FACILITY OVERVIEW

The test facility at the University of Sussex consists of a two stage axial turbine test section, rated to 400 kW, with an engine representative geometry, at an overall design pressure ratio of approximately 2.7:1. Hot main annulus air is supplied to the test section by an adapted Rolls Royce DART 3 MW aero engine. The air passes through a settling chamber and bellmouth to reduce pressure asymmetry and swirl in the test section. A hydraulic dynamometer and 3:1 reduction gearbox are used to absorb the power transmitted by the turbine.

Cooling air is supplied to the test section via an Atlas Copco ZT250 oil free compressor. Flow control valves allow adjustments of +/- 0.1 gs^{-1} to be made during a test run. Both the annulus flow and cooling flow lines are insulated. The stationary components of the test section contain 73 K-type thermocouples at various locations including both metal and air measurements. The rotating assembly contains 81 K-type thermocouples at 27 distinct locations. A Datatel radio telemetry system provides non-contact transmission of the signals.

The rig includes a number of pressure measurements, which are used to monitor main annulus conditions and aid in the balancing of cooling system seals. The accuracy obtained after calibration is within 0.017 % of span for 0 to 3.5 bar.

The cooling air supplied to the rig, including both the main cooling flow and the balance flow, as well as the seal vent air coming from the rig are measured by hot film flow meters. These were calibrated to an accuracy of +/- 1.3 % for the range of mass flow for intended measurements. The main annulus mass flow is measured using an upstream venturi.

Figure 2 shows the major dimensions of the test section (at the request of industrial partners these have been non-dimensionalised). The dimensions are presented in terms of h, the radial distance from the rotor shaft to the outer radius of the main annulus.

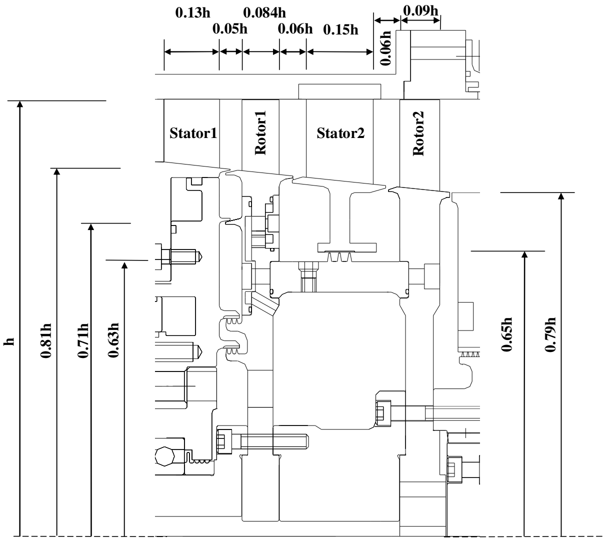

Figure 2: Test section geometry

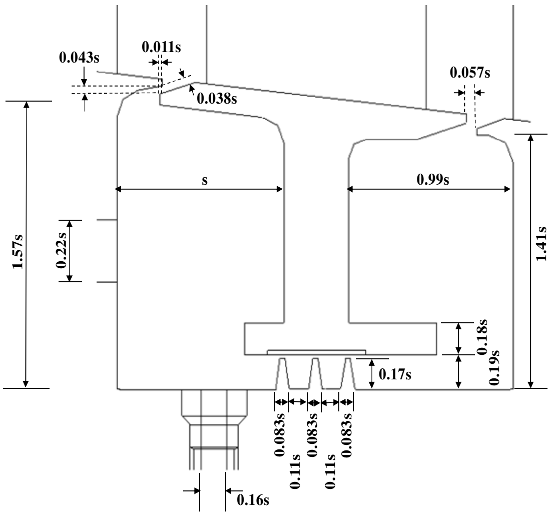

Figure 3: Stator well and seal dimensions

Figure 3 shows the stator well dimensions, including the major dimensions of the interstage seal and the upstream and downstream rim seals. The dimensions are presented in terms of s, the upstream rotor-stator spacing. Table 1 gives the blade and nozzle parameters of each stage.

	Stator 1	Rotor 1	Stator 2	Rotor 2
Pitch/Chord	0.6806	0.7791	0.7301	0.7512
Height/Axial Chord	1.199	2.188	1.233	2.568
Inlet Mach number	0.1885	0.2763	0.2570	0.3014
Exit Mach number	0.6563	0.6001	0.6529	0.6143
Inlet flow angle (^{o})	0.00	36.68	19.02	23.32
Exit flow angle (^{o})	70.07	65.36	64.60	59.33

Table 1: Blade and nozzle parameters

EXPERIMENTAL OBJECTIVES

The GC measurements on the turbine stator well rig are designed to satisfy two measurement objectives:

i) Obtain measurements of main annulus rim seal exchange
ii) Obtain measurements of flow re-ingested into the stator well cavities

The measurement of the rim seal exchange was conducted with geometry used as part of the cooling effectiveness studies. The re-ingestion experiment however required a bespoke geometry to be tested where the coolant delivery paths to the stator well were blocked.

GAS CONCENTRATION INSTRUMENTATION

The development of the GC measurement system used for the experiments described here required a dual species gas delivery, sample handling and measurement system. The system can be seen in Figure 4. Carbon dioxide was selected due to its non corrosive property, having no detrimental effect on the rig or piping materials. The carbon dioxide is delivered from a 25 kg supply at 50 bar.

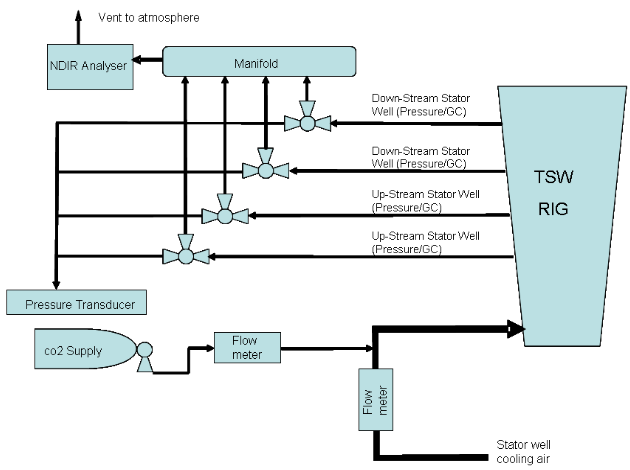

Figure 4: Gas concentration delivery and measurement system

The carbon dioxide passes through an inline heater to ensure the gas delivery temperature to the seeding supply flow meter is within +/- 10 K of temperature at which the meter was calibrated. This results in a seeding flow rate uncertainty of +/- 0.01 gs^{-1}. The metered seeding gas is then introduced to the main cooling supply flow to provide a homogeneous gas mixture. Gas samples are taken from four locations within the rig, two located in the upstream wheelspace and two in the downstream wheelspace, each located at r = 0.905b. The locations can be seen in Figure 5. The gas samples are taken at a flow rate of less than 0.002 $C_{W,\ ENT}$ which approached isokinetic conditions. Each of the sampling locations are pressure taps during normal running of the rig. A solenoid system allows the measurement to be switched between gas sampling or pressure measurement. When the solenoids are in the position to allow gas samples, the gas is piped to the gas analyser. The gas analyser consists of two NDIR infrared units run in series, having ranges of 0-1% and 0-10% carbon dioxide content by volume. Due to the transport time of the gas through the system the measurements are time averaged values.

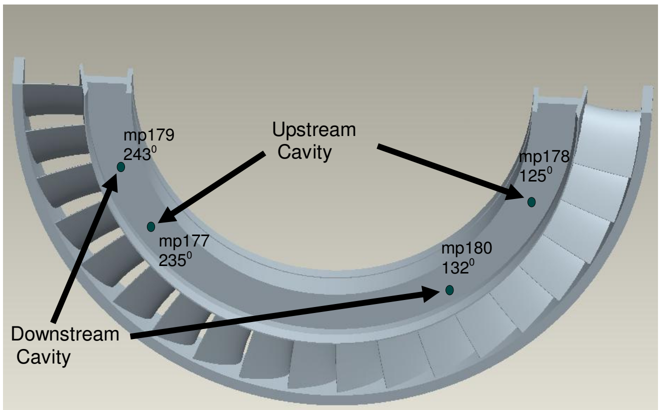

Figure 5: Upstream and downstream GC measurement locations

MEASUREMENT VALIDATION

Before the installation of the instrumentation on the TSW rig an external test was undertaken to prove the measurement method. Metered ambient air was supplied to a length of pipe. A known mass flow of carbon dioxide was then used to seed the ambient air. Both of these mass flows were measured using the flow meters to be used in the rig. A sample of the gas mixture was then taken 100 diameters downstream to ensure fully mixed flow, which was then passed to the gas analysers. The measured concentration was compared to the ideal concentration calculated from the known mass flows of air and carbon dioxide introduced to the pipe. This was repeated with a variety of air to carbon dioxide ratio's of rates expected within the TSW rig. The measured data was found to be within 1% of the calculated data across the seeding range.

Once installed in the TSW rig the entire GC seeding and sampling system was tested on the rig. The test was conducted with the rotating assembly stationary and with the rig inlet and outlet closed. This allowed the rig to be pressurised, giving a pressure drop from the rig to the gas analysers of the magnitude that would be seen during a full test matrix run. This also ensured a homogenous mix of ambient air to carbon dioxide throughout the TSW rig. As with the pipe test a metered amount of ambient air and carbon dioxide seeding gas was then supplied to the TSW rig. This was supplied via the main cooling air path. Once the pressure in the rig had reached the desired level, samples were taken from the rig measurement points. The test was conducted at three seeding flow rates. For each condition the measurement points showed the sampling system to give repeatable results within 2%. This represents the uncertainty of the system.

RIM SEAL EXCHANGE EXPERIMENTS

The rim seal exchange experiments were designed to provide information on the interaction of main annulus and cooling air across the upstream stator well rim seal. The gas flows being investigated are shown in Figure 6. For these experiments, coolant with a known concentration of carbon dioxide was introduced to the test section through either drive arm holes or simulated lock plate slots. Concentration measurements in the stator well were then made. From the supplied and measured concentration, a dilution ratio is calculated. This, together with a known interstage seal flow can be used to calculate the net rim seal exchange. Due to the pressure ratio of the downstream stator well to the main annulus it is assumed that the there is no/minimal ingress through the downstream stator well rim seal. Therefore gas samples taken from the downstream cavity give the concentration of the gas mixture which has passed through the interstage seal and therefore can be used to inform concentration measurements taken upstream of the interstage seal.

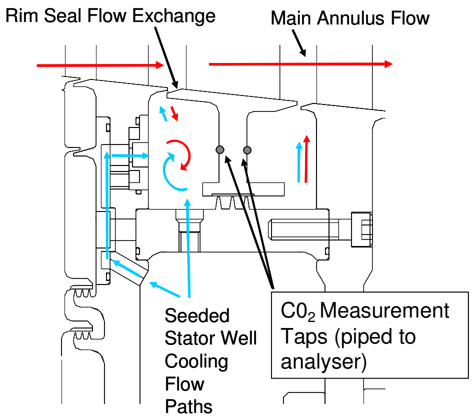

Figure 6: Rim seal exchange experimental flows

Although it would be possible to measure the coolant delivery rate, calculate the interstage seal flow and from summation alone determine an average rim seal flow, this would not take into account the possibility of a rim seal exchange. The technique used here was developed to overcome the inherent uncertainties of a direct summation approach to determining the rim seal flow. The difference in the concentration measured in the stator wells as compared to the delivery rate allows the total amount of main annulus air entering the stator well to be calculated. Where the addition of this value to the supplied cooling flow exceeds the interstage seal flow, a rim seal exchange is indicated. This is demonstrated graphically in Figure 7, where both techniques are compared.

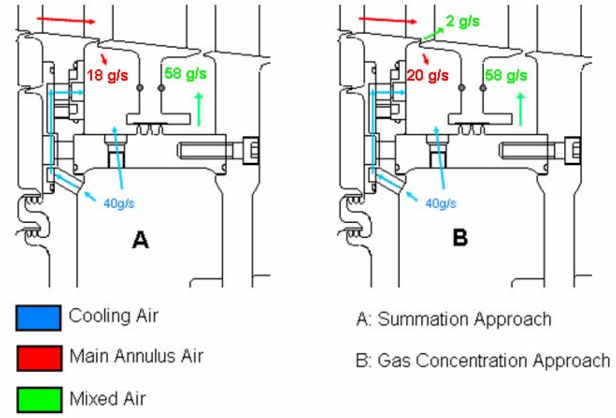

Figure 7: Comparison of summation and gas concentration techniques for quantifying rim seal exchange

For case A, a know cooling flow rate of 40 gs^{-1} has been used in conjunction with a known seal flow of 58 gs^{-1} to estimate the net ingestion of 18 gs^{-1}. This approach is limited by the assumption that the rim seal flow is uni-directional. B, where the cooling flow and seal flow are of the same magnitude, with the addition of GC measurements in the cavity, takes into account the rim seal exchange where pressure asymmetries allow bi-directional flow through the seal. If the GC measured was in the region of 66% of the supplied coolant concentration, giving a dilution ratio of 0.66, this would suggest around 20 gs^{-1} ingress. A summation of the flows would then show that 2 gs^{-1} is egressing through the rim seal back into the main annulus. This is shown in the following analysis. The carbon dioxide is mixed with the cooling air before entering the test section. The total mass flow rate is then calculated.

$$\dot{m}_{SC} = \dot{m}_C + \dot{m}_{SG} \qquad \textbf{Equation 5}$$

From the known mass flows of carbon dioxide and cooling air the concentration of the supplied coolant is calculated, taking into account the ambient carbon dioxide level.

$$GC_{SC} = \left[\left[\frac{100}{\dot{m}_{SC}}\right] \times \left\{\dot{m}_{SG} + \left[\left[\frac{\dot{m}_C}{100}\right] \times Ambient\ CO_2\right]\right\}\right] \qquad \textbf{Equation 6}$$

From the calculated delivery concentration and the concentration measured in the stator well a dilution ratio is calculated.

$$DR = \left[\frac{GC_{SW}}{GC_{SC}}\right] \qquad \textbf{Equation 7}$$

The dillution ratio is then used to calculate the total flow into the cavity, which includes the supplied coolant and ingested main annulus gas.

$$\dot{m}_{USW} = \left[\frac{\dot{m}_{SC}}{DR}\right] \qquad \textbf{Equation 8}$$

From this value, the rim seal exchange values for seal ingress and egress can be calculated.

$$\dot{m}_{ING} = \dot{m}_{USW} - \dot{m}_{SC} \qquad \textbf{Equation 9}$$

$$\dot{m}_{EGR} = \dot{m}_{USW} - \dot{m}_{IS} \qquad \textbf{Equation 10}$$

RE-INGESTION EXPERIMENT

Quantifying the re-ingestion of coolant gas is often difficult or impossible with temperature and pressure measurements alone. The main obstacle to this measurement is differentiating between re-ingested and normally supplied cooling air to a cavity. In order to address this, a specific experiment was devised. This is shown in Figure 8. Both the drive arm holes and simulated lock plate slots were blocked ensuring the direct coolant supply paths to the stator-well cavity were closed. The upstream wheelspace was then supplied with seeded cooling air.

With the rig in this configuration, all the seeded cooling flow passes up the wheelspace and directly into the main annulus flow. This ensures that the only path for coolant to reach the stator-well is by re-ingested from the main annulus. The data reduction equations are outlined below.

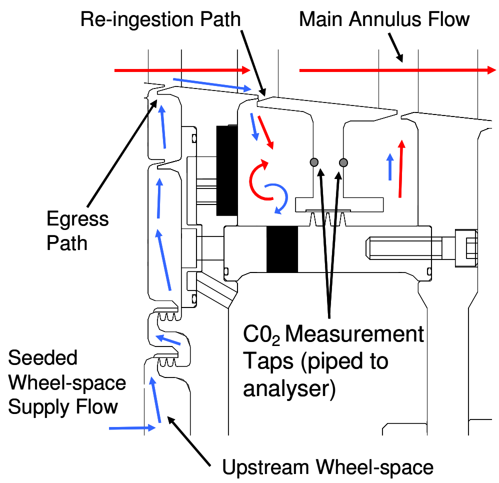

Figure 8: Re-ingestion experimental flows

Cooling air seeded with a known mass of carbon dioxide is supplied to the upstream wheelspace. The total wheelspace supply is calculated from these measured values.

$$\dot{m}_{WS} = \dot{m}_C + \dot{m}_{SG} \qquad \textbf{Equation 11}$$

The concentration of the wheelspace supply can then be calculated.

$$GC_{WS} = \left[\left[\frac{100}{\dot{m}_{WS}} \right] \times \left\{ \dot{m}_{SG} + \left[\left[\frac{\dot{m}_C}{100} \right] \times Ambient\ CO_2 \right] \right\} \right] \qquad \textbf{Equation 12}$$

Concentration measurements are then taken in the stator wells. As the coolant delivery paths are blocked total rim seal ingress into the upstream stator well is equal to the interstage seal flow.

$$\dot{m}_{USW} = \dot{m}_{IS} \qquad \textbf{Equation 13}$$

The ratio of the supplied wheelspace coolant flow concentration and the measured stator-well concentration can then be calculated.

$$DR = \left[\frac{GC_{SW}}{GC_{WS}} \right] \qquad \textbf{Equation 14}$$

The wheelspace flow which has been re-ingested into the upstream stator-well can then be calculated.

$$\dot{m}_{RE} = \dot{m}_{USW} \times DR \qquad \textbf{Equation 15}$$

INTERSTAGE LABYRINTH SEAL FLOW ESTIMATION

The TSW interstage labyrinth seal is a three fin straight through seal with a 0.3 mm cold build clearance, set so that the seal demand is lower than disc entrainment flow and coolant delivery. It will be shown later that the hot running clearance is 0.4 mm. This results in a clearance that is scaled down from typical engine values, giving low rotational Reynolds numbers when compared too much of the data in open literature. For the purpose of this work, the 2D, non-rotating data of Wittig *et al.* [8] has been used to estimate a C_D. Their tightest clearance tested, 0.5 mm, (together with 2.5, 1.5 and 1.0 mm) is close to the TSW seal and the geometry is similar. Specifically, the estimation of the C_D value has been derived from an extrapolation of the 6 and 1 fin data, too 0.3 mm clearance. An estimate for the 3 fin C_D was derived from the numerical modeling of the Wittig *et al.* data by Kim and Cha [16]. Equivalent 2, 3, 4 and 5 fin predictions were made together with the 1 and 6 fin cases. Based on their results, the 3 fin C_D is expected to be approximately 45 % worse than the 6 fin value in comparison to the single fin datum, which gives a C_D estimate of 0.48.

Figure 9 shows a comparison of seal flows calculated using a C_D of 0.48 with the St. Venant-Wantzell equation, with seal flow results from CFD. The pressure ratio is the upstream to downstream seal pressure. The normalized seal flow is seal flow / $C_{W,\ ENT}$. The CFD results are within 2% of the calculated values. The effect of rotation has been shown to reduce the discharge coefficient. The TSW seal is at the borderline between the axial and rotationally affected regimes, so the effect is not expected to be significant.

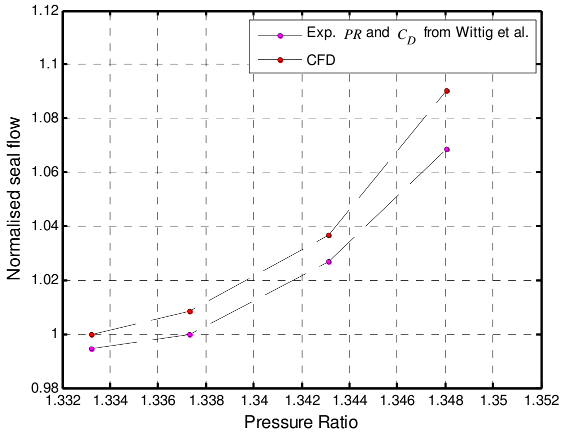

Figure 9: Comparison of CFD predicted seal flows with calculated seal flows using C_D of 0.48, for upstream to downstream seal pressure ratios of 1.333 to 1.348

DISPLACEMENT INSTRUMENTATION

An experimental method was devised to measure hot running geometry changes using eddy current displacement sensors. The sensor locations are shown in Figure 10. A sensor for measuring axial movement in the rig is located downstream of rotor 2, while a second sensor is located on the stator foot downstream of the interstage seal. This sensor measures the change in radial gap of the seal which is of particular importance when quantifying interstage seal flows. The space available and operating environment dictated that a non contact system was essential, which removes the possibility of contact errors and frictional heating of the measurement surface.

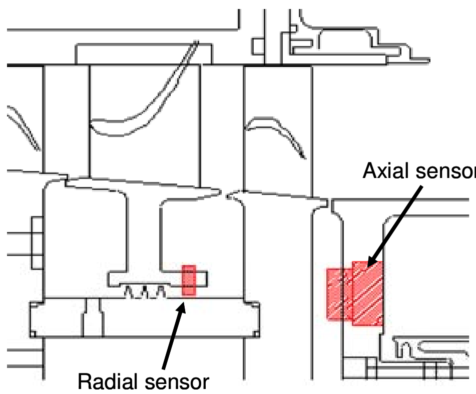

Figure 10: Displacement sensor locations

It was necessary to complete the sensor calibration before rig assembly, meaning the sensors could not be calibrated whilst subject to operating temperature and pressure. In order to quantify the possible uncertainty of calibrating at ambient conditions rather than operating conditions an isothermal box was created in which each sensor could be placed and output changes due to changes in temperature measured. For each sensor the resultant measurement uncertainty due to temperature change from ambient to operating temperature was less than the dynamic resolution of the sensor.

Figure 11: Radial sensor and target calibration

The radial sensor was calibrated located in its operational position downstream of the interstage seal in the stator hub. A target of the same geometry and material as the drive arm was then used to give sensor readings for three displacement values, this setup can be seen in Figure 11. The sensor outputs were found to be repeatable to within +/- 0.02 V, corresponding to a measurement uncertainty of +/- 0.001 mm over the 0.5 mm range.

Data from the radial sensor gives a direct measurement of the net interstage seal movement. Figure 12 shows the seal movement for a typical rig commissioning run as well as the associated rig speed. Stator and rotor temperatures for the run are also shown. The cooling flow rate has been kept constant so that the dominant factor in the increasing rig temperatures seen are the result of increasing hot main annulus flow. As the rig begins to rotate an initial spike is seen in the seal gap as the blades load and the rotating assembly settles (point a). The seal gap can then be seen to close as the stator temperatures initially drop (point b). However the gap then begins to open as rig temperatures increase (point c). The stator material has a coefficient of thermal expansion almost 40% greater than that of the rotor material. The higher radius part of the seal where the sensor is mounted therefore expands more than the lower radius rotating part of the seal despite the similar temperature of the rotor and stator at a similar radius to the seal. The seal gap can then be seen to settle once the temperatures stabilise (point d).This pattern can be seen to repeat with each speed increase up to 10,000rpm where the seal gap has increased by 0.1mm (point e). The seal cold build clearance of 0.3mm has therefore seen an increase of 33% highlighting the importance or accurately predicting the hot geometry of such seals and the influence on the flows within the stator well. At the end of the run, a sudden increase in seal gap is seen as the main annulus supply is removed and the rotating assembly slows (point f). At this point any centrifugal growth has been removed causing the rotating assembly to reduce in radius, moving away from the stationary assembly. The gap then begins to close up as the rig rapidly cools (point g).

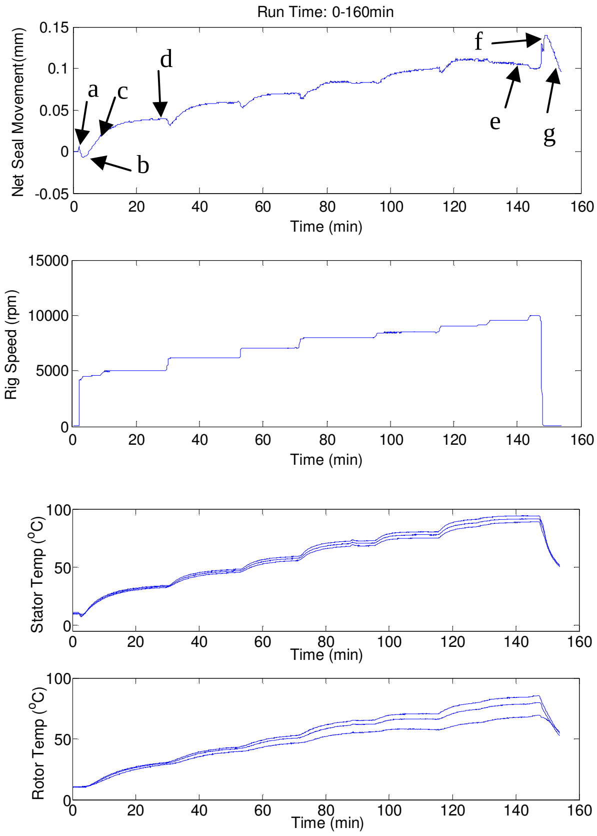

Figure 12: Radial sensor output, rotational speed and rotor-stator temperatures for a full test cycle

THERMO-MECHANICAL MODELLING

The radial sensor was not installed for the duration of the test matrix. In order to provide seal clearance values across the TSW test matrix, a thermo-mechanical modeling capability has been developed. A model constructed using the Rolls-Royce in-house code SC03, was matched thermally by using test data temperatures to inform model boundary conditions. The resulting seal movement was then compared to the experimental values of displacement taken from the radial sensor.

Data is shown in Figure 13 for the measured rig and modeled clearance values. The FEA model points, shown as red crosses are single data points where the model has been matched to the rig speed and temperatures. The model was found to predict the change of seal clearance to within 0.009 mm.

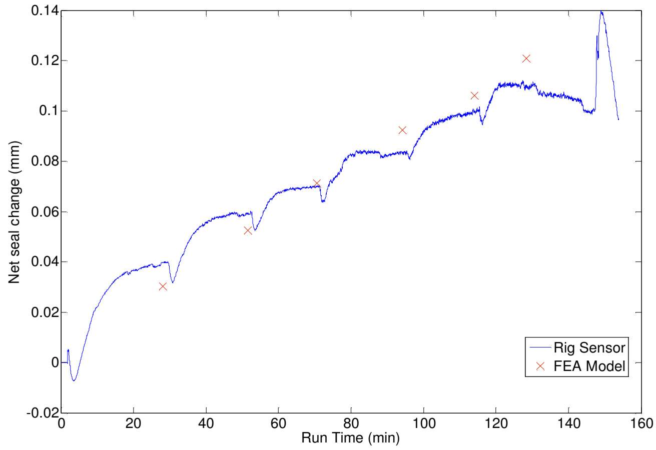

Figure 13: Comparison of measured and modeled net seal movement

RIM SEAL EXCHANGE EXPERIMENTAL RESULTS

Rim seal exchange GC measurements were taken with four rig geometries at cooling flows of 0.77 $C_{W,\,ENT}$ and 1.04 $C_{W,\,ENT}$ corresponding to in cavity rotational Reynolds numbers of $1.76\text{x}10^6 < Re_\varphi < 1.86\text{x}10^6$. The four geometries studied, including 26 and 39 drive arm holes and 26 and 39 simulated lock plate bleed slots, are shown in Figure 14.

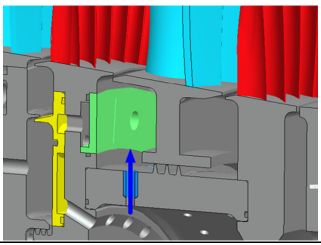	**Geometry 1:** 39 drive arm holes, equal circumferential spacing, without lock plate bleed slots
	Geometry 2: 26 drive arm holes, equal circumferential spacing, without lock plate bleed slots
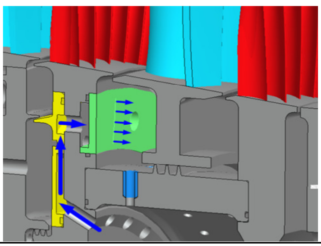	**Geometry 3:** 39 lock plate bleed slots equal circumferential spacing, without drive arm holes
	Geometry 4: 29 lock plate bleed slots equal circumferential spacing, without drive arm holes

Figure 14: Cooling supply geometries

The dilution ratios for the four measurement locations for both drive arm configurations are shown in Figure 15. A dilution ratio of zero indicates that no seeded cooling air is present, a ratio of 1 indicates that no main annulus air is present. For both drive arm hole configurations at 0.77 $C_{W,\,ENT}$ a large variation was seen between the measurements taken in the upstream wheelspace and the measurements taken in the downstream wheelspace. The lower dilution ratio in the upstream wheelspace indicates that the cooling air has not fully mixed with main annulus ingress into the cavity. The higher ratio in the downstream cavity suggests the cooling air directly feeds the interstage seal, so a higher concentration is measured in the downstream cavity.

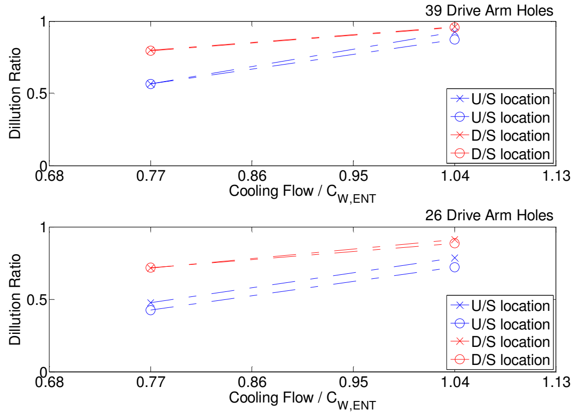

Figure 15: Measured dilution ratios for 39 and 26 drive arm holes, at cooling flow rates of 0.77 $C_{W,\,ENT}$ and 1.04 $C_{W,\,ENT}$, $1.76\text{x}10^6 < Re_\varphi < 1.86\text{x}10^6$

The dilution ratios for the measurement locations at 1.04 $C_{W,\,ENT}$ show a similar effect, where the dilution ratio is lower for the upstream cavity. However the difference is greatly reduced when compared to 0.77 $C_{W,\,ENT}$. This suggests that with increased cooling flow the coolant has more fully mixed at the upstream measurement locations, cooling at a higher radius in the cavity. This increase in cooling effectiveness at higher cavity radius is in agreement with the findings of Coren *et al.* [1] which indicated cavity sealing in the vicinity of 1.04 $C_{W,\,ENT}$.

Figure 16 shows stator well streamlines from a CFD study of the 39 drive arm hole geometry for two coolant flow rates of 0.58 $C_{W,\,ENT}$ and 0.77 $C_{W,\,ENT}$. For 0.58 $C_{W,\,ENT}$, where the supplied coolant flow rate is much lower than the disc entrainment it can be seen that the coolant does not penetrate to the higher radius areas of the stator well but directly feeds the interstage seal. For 0.77 $C_{W,\,ENT}$ the coolant has penetrated into the cavity. A detailed overview of this study can be found in Coren [15].

Comparison of the downstream measurement locations, where the sampled gas has more completely mixed for both flow rates, shows that the dilution ratio increases with increased coolant flow. This indicates that for the higher coolant flow rate the upstream cavity has been more effectively sealed reducing the ingress of hot main annulus gas through the rim seal. The results also suggest generally worse sealing with fewer delivery holes. This is not yet fully understood

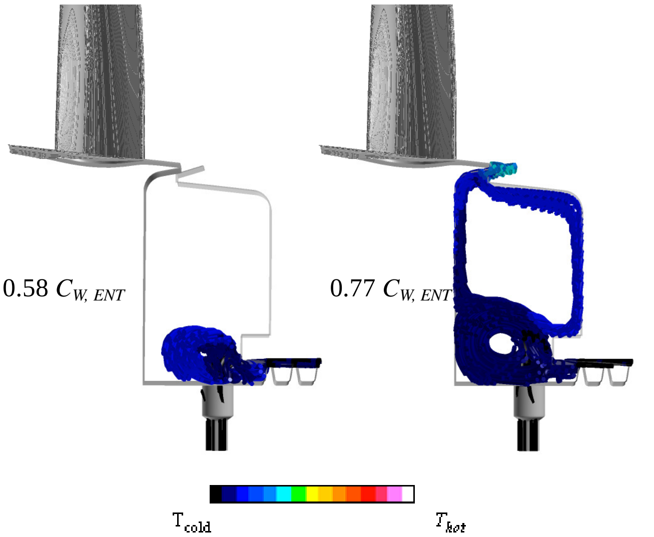

Figure 16: Cavity streamlines for drive arm configuration coloured by normalised absolute frame total temperature, interstage seal flow = 0.9 $C_{W, ENT}$

The dilution ratios for the four measurement locations, shown in Figure 5, for both lock plate slot configurations are shown in Figure 17. The results for the lock plate slot geometries showed much closer agreement between the dilution values seen for the upstream and downstream measurement locations for 0.77 $C_{W, ENT}$ and 1.04 $C_{W, ENT}$. This suggests that with lock plates the coolant has mixed fully with ingested main annulus air in both cavities as opposed to the drive arm geometries where the coolant had not fully mixed in the upstream cavity. This is due to the coolant being fed directly into the disc entrainment This result indicates that the introduction of the cooling air through the lock plate slots has increased the amount of coolant present at the higher radius areas of the upstream stator well. This result is corroborated by the findings of Coren *et al.* [15] which indicate greater upstream cavity mixing with lock blade bleed slots when compared to drive arm hole delivery. As with the dilution ratios obtained for the drive arm tests, the ratios obtained for both the 26 and 39 lock plate slot geometries show an increased concentration measurement for the higher cooling flow. This shows that the higher cooling flow has reduced the ingress of main annulus gas into the upstream cavity. As expected for both 26 and 39 lock plate slots the dilution ratio is within 0.05 of being equal to 1, showing minimal ingestion through the rim seal.

The increased sealing of the cavities for both the drive arm and lock plate slots shown by the concentration measurements are supported by the temperature measurements discussed in Coren *et al.* [15]. Cooling effectiveness was seen to increase with increased cooling flow. Temperature measurements also support the findings from the lock plate slot tests where coolant is thought to have penetrated further into the cavity and increased cooling on the stator face when compared to similar flow rates through drive arm hole geometries.

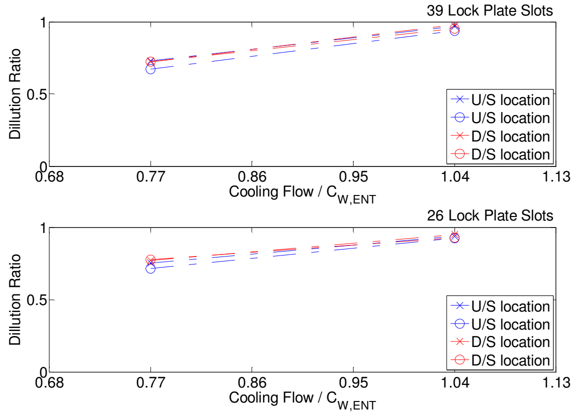

Figure 17: Measured dilution ratios 39 and 26 lock plate slots, at cooling flow rates of 0.77 $C_{W, ENT}$ and 1.04 $C_{W, ENT}$, $1.76x10^6 < Re_\varphi < 1.86x10^6$

Figure 18 shows the rim seal exchange for 39 lock plate slots as calculated by the method discussed earlier. The flows are presented as fractions of the interstage seal flow. By a direct summation approach the difference between the interstage seal flow and the supplied cooling flow would indicate ingress of around 0.1 IS. However the concentration measurement method indicated almost 0.2 IS enters the cavity, but that 0.1 IS is then egressed rather than passing through the interstage seal.

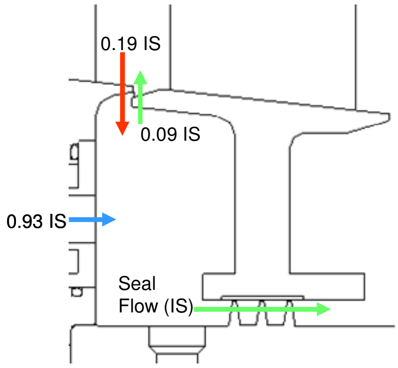

Figure 18: Rim Seal Exchange for 39 lock plate slots, flow rates expressed as fractions of the interstage seal

RE-INGESTION EXPERIMENTAL RESULTS

The re-ingestion experiment was conducted at three wheelspace egress rates, where Re_φ=1.65x10^6. This value is lower than would be expected under normal rig conditions due to the lack of cooling air being directly supplied to the rotor stator cavity. Results are shown in Figure 19. These results are based upon interstage seal flows calculated with a hot running clearance calculated using the FEA model previously discussed and a C_D of 0.5, the C_D value being increased from

0.48 to account for the increase in seal area under hot running conditions. The interstage seal flow calculated using predicted hot geometry showed an increase of almost 27% when compared to cold geometry calculations. The egress and re-ingestion rates are shown as fractions of interstage seal flow.

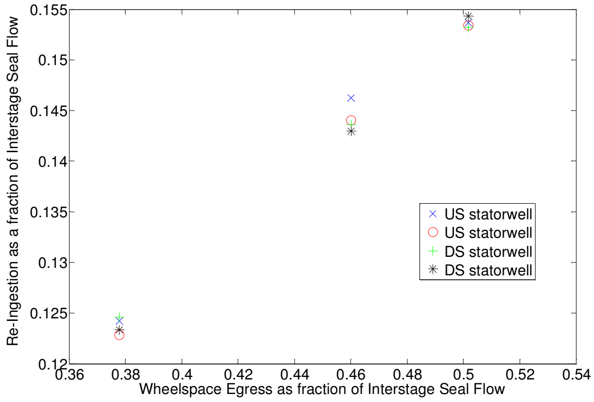

Figure 19: Measured re-ingestion rates for wheelspace egress rates of 0.37IS to 0.51IS, Re_{φ}=1.65x10^6

Figure 20 shows the percentage of wheelspace egress which is re-ingested into the stator cavity against the egress rate, where the egress rate is given as a fraction of the main annulus flow. It can be seen that although re-ingestion increases with increased egress the percentage of the re-ingestion decreases.

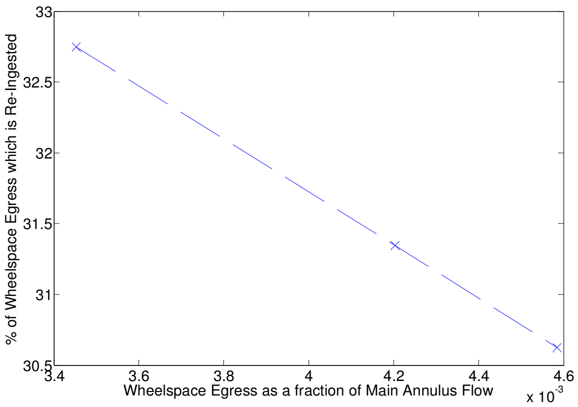

Figure 20: Percentage re-ingestion rates for wheelspace egress expressed as a fraction of main annulus flow, Re_{φ}=1.65x10^6

Figure 21 shows a CFD solution displaying streamlines which are seeded at the point of egress from the wheelspace. The wheelspace has not been modeled. The streamlines suggest that the coolant would be initially entrained directly on to the blade foot boundary layer. The low momentum of the fluid causes it to be drawn up onto the blade suction surface as the gas approaches the tail of the blade and mixes with secondary flows. As such it is likely the coolant begins to lift from the foot in to the main annulus. This results in pockets of mixed coolant and main annulus gas and areas of pure main annulus gas above the rim seal. The gas re-ingested into the stator well is drawn from these two gas mixtures. The reduction in percentage re-ingestion with increased egress indicates that more coolant is mixing with the main annulus air as the momentum of the coolant through the wheelspace rim seal increases, which simply reduces the concentration at the rim seal.

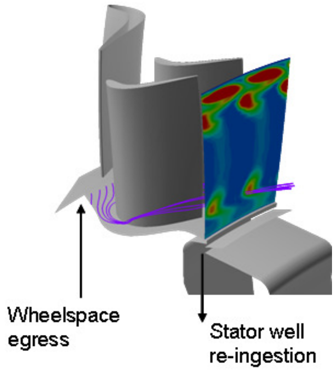

Figure 21: Streamlines of wheelspace egressed coolant

CONCLUSIONS

A two stage turbine rig with a shrouded second stage has been used to investigate ingestion in a turbine stator well. The rig enables investigation of coolant supplied by means of both coolant supply holes in the drive arm as well as coolant supplied by means of lock plate bleed slots. A non-invasive technique using tracer gas seeding and detection together with displacement sensors has been developed to provide measurements of rim seal exchange flows and re-ingestion flows within a engine representative test rig. Dilution ratio data from GC measurements has shown that as the cooling flow rate in the stator well increases, the coolant mixes more fully in the upstream stator well, providing more effective cooling at a higher radius with an effective reduction of the ingress of hot main annulus gas through the rim seal. At low flow rates the coolant is thought to pass straight through the interstage seal. Re-ingestion experiments have indicated that the percentage of wheelspace re-ingested is in the region of 30% for the range of realistic coolant flow rates explored, with the re-ingestion reducing with increasing coolant flow. The GC results can be used to determine the sealing effectiveness of a number of coolant flow rates. The data is suitable for the progression and validation of modern conjugate/coupled analysis tools.

ACKNOWLEDGEMENTS

The present investigations were supported by the European Commission within the Framework 6 Programme, Research Project 'Main Annulus Gas Path Interactions (MAGPI)', AST5-CT-2006-030874. This financial support is gratefully acknowledged. The authors would like to thank J. A. Dixon (Rolls Royce Plc) and J. R. Turner. Thanks are also given to Simon Davies, Glenn Downs and Tony Martin for their assistance in the construction of the facility.

REFERENCES

[1] Coren, D. D., Atkins, N. R., Turner, J.R., Eastwood, D., Davies, S. Childs, P. R. N., Dixon, J. A., Scanlon, T. S., 2010, “An Advanced Multi-Configuration Stator Well Cooling Test Facility”. Proceedings of ASME Turbo Expo 2010, Paper Number GT2010-23450.

[2] Daily, J. W., Nece, R. E., 1960, “Chamber Dimension Effects on Induced Flow and Frictional Resistance of Enclosed Rotating Discs”. Journal of basic engineering, Vol.82., pp.217-232.

[3] Chew, J. W., 1998, “The Effect of Hub Radius on the Flow Due to a Rotating Disc” Journal of Turbomachinery, Vol. 110, pp. 417-418.

[4] Dorfman, L. A., 1963,”Hydrodynamic resistance and the heat loss of rotating solids”, Oliver & Boyd.

[5] Owen, J.M., Phadke, U.K., 1980, “An Investigation of Ingress for a Simple Shrouded Rotating Disc System with a Radial Outflow of Coolant”, ASME Paper 82-GT-145.

[6] Zimmermann, H., Wolff, K.H., 1998, Air System Correlations, Part 1: Labyrinth Seals, ASME Paper 98-GT-206.

[7] Gamal, A.M., Vance, J.M., 2007, Labyrinth Seal Leakage Tests: Tooth Profile, Tooth Thickness, and Eccentricity Effects, ASME Paper GT2007-27223.

[8] S. Wittig, U. Schelling, S. Kim, and K. Jacobsen, 1987, "Numerical predictions and measurements of discharge coefficients in labyrinth seals," ASME, International Gas Turbine Conference and Exhibition, 32nd, Anaheim, CA, 1987, p. 1987.

[9] Gentilhomme, O., Hills, N., and Turner, A. B., 2003. “Measurement and analysis of ingestion through a turbine rim seal”. ASME Journal of Turbomachinery, Vol. 125, pp. pp.505–512.

[10] Georgakis, C., Whitney, C., Woolatt, G., Stefanis, V., Childs, P., 2007, “Turbine stator well studies: Effect of upstream egress ingestion,” ASME paper GT2007-27406.

[11] Phadke, U. P., Owen J. M., 1988 “Aerodynamic Aspects of the Sealing of Gas Turbine Rotor-Stator Systems Part 1: The Behavior of Simple Shrouded Rotating-Disc Systems in a Quiescent Environment”. Int. J. Heat Fluid Flow, 9, pp. 98-105.

[12] Dadkhah, S., Turner, A, B., Chew, J. W., 1992 “Performance of Radial Clearance Rim Seals in Upstream and Downstream Rotor-Stator Wheelspaces”. ASME Journal of Turbomachinery, Vol. 114, pp.439–445.

[13] Green, T., Turner, A, B., 1994 “Ingestion Into the Upstream Wheelspace of an Axial Turbine Stage”. ASME Journal of Turbomachinery, Vol. 116, pp. 327-332.

[14] Dunn, D.M., Zhou, D.W., Saha. K., Squires. K.D., Roy. R.P., Kim. Y.W., Moon. H.K., 2010, “Flow Field in a Single-Stage Model Air Turbine Rotor-Stator Cavity with Pre-Swirled Purge Flow”. Proceedings of ASME Turbo Expo 2010, Paper Number GT2010-22869.

[15] Coren, D. D., Atkins, N. R., Long, C.A., Eastwood, D., Childs, P. R. N., Guijarro-Valencia,. A., Dixon, J. A., 2011, “The Effect of Stator Well Coolant Delivery Passage Configurations on Cooling Effectiveness”. Proceedings of ASME Turbo Expo 2011, Paper Number GT2011-46448.

[16] Kim, T. S., Cha, K. S., 2009, “Comparative analysis of the influence of labyrinth seal configuration on leakage behavior”. Journal of Mechanical Science and Technology 23 (2009) 2830~2838.